

Modern Physics Letters A
 © World Scientific Publishing Company

DARK MATTER DYNAMICS AND INDIRECT DETECTION

GIANFRANCO BERTONE

*NASA/Fermilab Particle Astrophysics Center,
 Batavia, IL 60510, USA
 bertone@fnal.gov*

DAVID MERRITT

*Department of Physics, Rochester Institute of Technology,
 54 Lomb Memorial Drive, Rochester, NY 14623, USA
 merritt@astro.rit.edu*

Non-baryonic, or “dark”, matter is believed to be a major component of the total mass budget of the universe. We review the candidates for particle dark matter and discuss the prospects for direct detection (via interaction of dark matter particles with laboratory detectors) and indirect detection (via observations of the products of dark matter self-annihilations), focusing in particular on the Galactic center, which is among the most promising targets for indirect detection studies. The gravitational potential at the Galactic center is dominated by stars and by the supermassive black hole, and the dark matter distribution is expected to evolve on sub-parsec scales due to interaction with these components. We discuss the dominant interaction mechanisms and show how they can be used to rule out certain extreme models for the dark matter distribution, thus increasing the information that can be gleaned from indirect detection searches.

1. Dark Matter Candidates and Constraints

If one compares the total amount of matter inferred from cosmic microwave background (CMB) experiments¹

$$\Omega_M h^2 = 0.135^{+0.008}_{-0.009}. \quad (1)$$

(here Ω denotes the mean density as a fraction of the critical, or closure, density, and h is the Hubble constant in units of $100 \text{ km s}^{-1} \text{ Mpc}^{-1}$) with the amount of baryons allowed by the CMB

$$\Omega_b h^2 = 0.0224 \pm 0.0009 \quad (2)$$

(also consistent with the Big Bang nucleosynthesis constraint $0.018 < \Omega_b h^2 < 0.023$, see *e.g.* Ref. 2), one is left with a component of the Universe that is composed of matter distinct from ordinary baryonic matter. There is no shortage of dark matter candidates, most of them arising in theories beyond the standard model of particle physics. In the framework of the standard model, neutrinos have been proposed as dark matter candidates, but the analysis of CMB anisotropies, combined with

large-scale structure data, suggest $\Omega_\nu h^2 < 0.0067$ (95% confidence limit), which implies that neutrinos are a sub-dominant component of non-baryonic dark matter.

Rather than compile a complete list of all possible dark matter candidates (often referred to as *WIMPs*: “Weakly Interacting Massive Particles”) we discuss here the candidates that have received the widest attention in the recent literature. For an extensive review of particle dark matter candidates see e.g. Refs. 3 and 4.

The *neutralino* in models of R-parity-conserving supersymmetry is by far the most widely studied dark matter candidate. In the “minimal supersymmetric standard model” (MSSM), the superpartners of the B and W_3 gauge bosons (or the photon and Z , equivalently) and the neutral Higgs bosons, H_1^0 and H_2^0 , are called binos (\tilde{B}), winos (\tilde{W}_3), and higgsinos (\tilde{H}_1^0 and \tilde{H}_2^0), respectively. These states mix into four Majorana fermionic mass eigenstates, called neutralinos. The lightest of the four neutralinos, commonly referred to as “the” neutralino, is in most supersymmetric scenarios the lightest supersymmetric particle. The neutralino is a perfect dark matter candidate, with mass and interaction cross sections that, in fine-tuned regions of the supersymmetric parameter space, can correctly reproduce the dark matter relic density while still being consistent with constraints on the WIMP mass and searches in accelerators as well as direct and indirect detection experiments.

Another interesting candidate arises in theories with universal extra dimensions (UED),⁵ i.e. extra-dimension scenarios in which all fields are allowed to propagate in the bulk. Upon compactification of the extra dimensions, all of the fields propagating in the bulk have their momentum quantized in units of $p^2 \sim 1/R^2$, where R is the compactification radius, appearing as a tower of states with masses $m_n = n/R$, where n labels the mode number. Each of these new states contains the same quantum numbers (charge, color, etc.) The *lightest Kaluza-Klein particle* (LKP) in the framework of UED, which is likely to be associated with the first KK excitation of the photon, or more precisely the first KK excitation of the hypercharge gauge boson,⁶ provides a viable dark matter candidate. We will refer to this state as $B^{(1)}$. The calculation of the $B^{(1)}$ relic density was performed by Servant and Tait,⁷ who found that if the LKP is to account for the observed quantity of dark matter, its mass (which is inversely proportional to the compactification radius R) should lie in the range 400 to 1200 GeV, well above any current experimental constraint.

Dark matter candidates are commonly believed to have masses in the range 1 GeV – 100 TeV. The lower value is the so-called Lee-Weinberg limit,^{8,9} while the upper value comes from the so-called unitarity bound.^{10,11} It is sometimes stated in the literature that the upper bound is of order 340 TeV. However, this comes from the now-obsolete requirement that $\Omega_M h^2 \lesssim 1$, adopted in 1989 by Griest and Kamionkowski.¹¹ If one instead adopts the modern estimate in Eq. (1), the upper limit on the mass of the dark matter particle is $m \lesssim 120\text{TeV}$.

These limits are, however, model-dependent. Light scalar particles with masses below 1 GeV are viable dark matter candidates,^{12,13} (referred to as *light dark matter* or alternatively *MeV dark matter*), since the Lee-Weinberg limit strictly

applies only to fermionic particles with standard model interactions. If MeV dark matter is to explain the 511 keV emission from the Galactic bulge observed by INTEGRAL,^{14,15,16} then a comparison of the inverse Bremsstrahlung emission (associated with dark matter annihilations into electron-positron pairs) with the diffuse Galactic background constrains the mass of the light dark matter particle to be smaller than ~ 20 MeV.¹⁷ It has been argued that hints of this scenario may also have been discovered in particle physics experiments¹⁸ and could have interesting implications for neutrino physics.¹⁹

The unitarity bound can also be violated if, e.g., dark matter particles were not in thermal equilibrium in the early Universe, but were instead produced via alternative mechanisms, such as gravitational production.^{20,21}

2. Halo Models

The probability of direct detection is proportional to the dark matter density in the solar neighborhood, and most discussions of indirect detection have also focussed on the Milky Way; in both cases, a model of the Milky Way's dark matter halo is crucial for predicting and interpreting event rates. Halo density profiles are usually derived from N -body simulations of gravitational clustering, which predict a characteristic form for $\rho(r)$, and on dynamical constraints like the Sun's orbital velocity, which provide a normalization. (For reviews, see Refs. 22 – 24.) The most recent and highest-quality N -body simulations^{25,26} suggest a universal dark-matter density profile of the form

$$\rho(r) \approx \rho_0 \exp \left[- (r/r_0)^{1/n} \right] \quad (3)$$

with $n \approx 5$;²⁷ the density normalization at the Solar circle implied by the Galactic rotation curve is $\rho \approx 0.3 \text{ GeV cm}^{-3} \approx 8 \times 10^{-3} M_\odot \text{pc}^{-3}$, with an uncertainty of a factor ~ 2 . Henceforth we refer to Eq. (3) with $\rho(R_\odot) = 0.3 \text{ GeV cm}^{-3}$ as the *standard halo model* (SHM). (Eq. 3 replaces the more approximate NFW model²⁸ in which the density is a single power-law, $\rho \sim r^{-1}$, inward of the Solar radius R_\odot .) Unfortunately the N -body simulations from which these halo models are derived have resolutions that are measured in hundreds of parsecs at best, whereas the signal from dark matter annihilations depends critically on the mass profile in the inner few parsecs of the Galaxy. Furthermore the N -body simulations typically ignore the influence of the baryons (stars, gas, etc.) even though these are known to dominate the gravitational potential of the inner Galaxy.

One simple, and probably highly idealized, way to account for the effect of the baryons on the dark matter is via *adiabatic contraction* models, which posit that the baryons contracted quasi-statically and symmetrically within the pre-existing dark matter halo, pulling in the dark matter and increasing its density.²⁹ When applied to a dark matter halo with the density law (3), the result is a halo profile with $\rho \sim r^{-\gamma_c}$, $\gamma_c \approx 1.5$ inward of the Solar circle and an increased density at R_\odot .^{30,31,32} Alternatively, strong departures from spherical symmetry – for instance, during the

mergers that created the Galactic bulge – might have resulted in *lower* dark matter densities in the inner tens of parsecs.^{33,34,35} However we argue below that the steeply-rising *stellar* density near the Galactic center makes such models unlikely, at least in the case of the Milky Way.

The annihilation signal from a region of volume V that includes the Galactic center is proportional to $\langle \rho^2 \rangle V$. For any $\rho \propto r^{-\gamma}$ with $\gamma \geq 3/2$, the small-radius dependence implies a divergent flux; hence the strength of an annihilation signal is crucially dependent on the dark matter distribution on very small scales, where neither the simulations nor the dynamical data provide useful constraints. In the following section we discuss physical arguments that can be used to constrain the dark matter distribution on these small scales, and in the final section we discuss the implications for indirect detection.

3. Dark-Matter Dynamics on Sub-Parsec Scales

At distances $r \lesssim 1$ pc from the Galactic center, the gravitational potential is dominated by stars and by the supermassive black hole (SBH). The stars are observed to have a density³⁶

$$\rho_\star(r) \approx 3.2 \times 10^5 M_\odot \text{pc}^{-3} (r/1\text{pc})^{-1.4}, \quad r \lesssim 5\text{pc}. \quad (4)$$

Estimates of the SBH’s mass range from $2 - 4 \times 10^6 M_\odot$,^{37,38,39}; the most recent estimates, based on the orbits of single stars, suggest $\sim 4 \times 10^6 M_\odot$, but for consistency with most pre-2005 papers on dark matter in the Galactic center, we here adopt $M_{bh} = 3.0 \times 10^6 M_\odot$. The gravitational influence radius r_h of the SBH (the radius containing a mass in stars equal to twice the SBH’s mass) is $r_h \approx 2$ pc. Within r_h , the dark matter distribution is likely to have been strongly affected by whatever processes resulted in the formation of the SBH and the nuclear star cluster, and by any subsequent interactions between dark matter and stars.

Fig. 1 shows a number of possible models for the dark matter density on sub-parsec scales. The standard halo model (SHM) discussed above, normalized to $\rho = 0.3 \text{ GeV cm}^{-3}$ at the Solar circle, predicts $\rho(r_h) \approx 10^{1.5} M_\odot \text{pc}^{-3}$. Allowing for adiabatic contraction of the dark matter by the baryons (§2) increases this by a factor of $\sim 10^2$, and the inner density slope $\gamma \equiv -d \log \rho / d \log r$ in this contracted model is ~ 1.5 or steeper, implying a divergent annihilation flux. But even steeper density profiles are possible. If the SBH grew in the simplest possible way – via slow, symmetrical infall of gas – the density of matter around it would also grow, in the same way that contracting baryons steepen the overall Galactic dark matter profile.^{40,41} This scenario predicts a final density (of stars or dark matter) near the SBH of

$$\rho(r) \approx \rho(r_{sp}) \left(\frac{r}{r_{sp}} \right)^{-\gamma_{sp}}, \quad \gamma_{sp} = 2 + \frac{1}{4 - \gamma_c} \quad (5)$$

with γ_c the dark matter density slope in the pre-existing “cusp,” i.e. the region $r \gtrsim r_h$.⁴² Such a *spike* in the dark matter density would extend inward from

$r_{sp} \approx 0.2r_h$,⁴³ and for $\gamma_c \gtrsim 1$, $\gamma_{sp} \gtrsim 2.3$ (Fig. 1). Now, the *stellar* density profile would respond in a similar way to growth of the SBH, and $\rho_*(r)$ is known to be shallower than $\rho_* \sim r^{-2.3}$ (Eq. 4). But this is probably a result of dynamical evolution that occurred after the SBH was in place (see below).

At even smaller radii, a limit to the dark matter density is set by self-annihilations: $\rho \lesssim \rho_a \equiv m/\langle\sigma v\rangle t$, with $t \approx 10^{10}$ yr the time since formation of the spike.⁴⁴ A strict inner cut-off to the dark matter density is set by the black hole's event horizon, $r_{Sch} = 2GM_{bh}/c^2 \approx 3 \times 10^{-7}$ pc for a non-rotating hole, although for reasonable values of m and $\langle\sigma v\rangle$, the density is limited by self-annihilations well outside of r_{Sch} (Fig. 1).

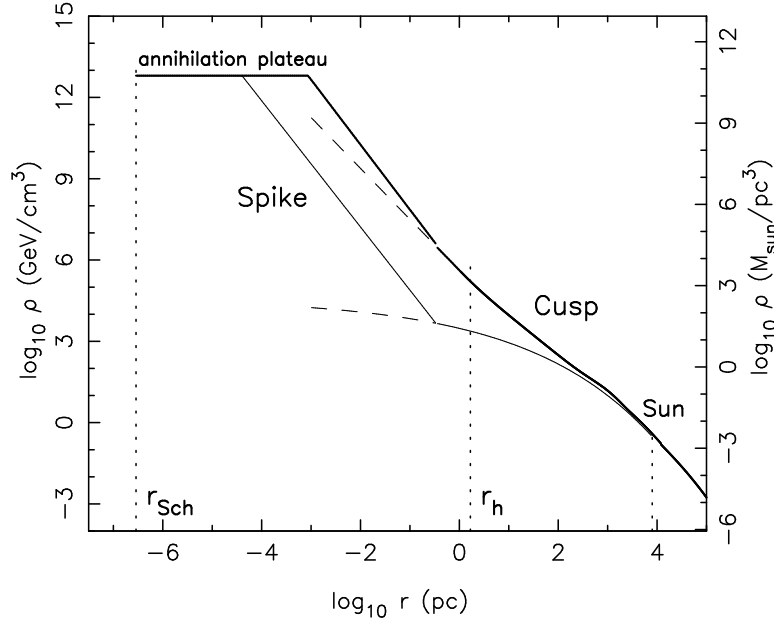


Fig. 1. Possible models for the dark matter distribution in the Galaxy. The thin curve shows the standard halo model (SHM), and the thick curve is the same model after “adiabatic compression” by the Galactic baryons (stars and gas). Both curves are normalized to a dark matter density of 0.3 GeV cm^{-3} at the Solar circle. Curves labelled “spike” show the increase in density that would result from growth of the Galaxy’s (SBH) at a fixed location. The annihilation plateau, $\rho = \rho_a = m/\langle\sigma v\rangle t$, was computed assuming $m = 200 \text{ GeV}$, $\langle\sigma v\rangle = 10^{-28} \text{ cm}^3 \text{ s}^{-1}$ and $t = 10^{10}$ yr. Dashed vertical lines indicate the SBH’s Schwarzschild radius ($r_{Sch} \approx 2.9 \times 10^{-7} \text{ pc}$, assuming a mass of $3.0 \times 10^6 M_\odot$ and zero rotation), the SBH’s gravitational influence radius ($r_h \approx 1.7 \text{ pc}$), and the radius of the Solar circle ($R_\odot \approx 8.0 \text{ kpc}$). Effects of the dynamical processes discussed in this article (scattering of dark matter off stars, loss of dark matter into the SBH, etc.) are excluded from this plot; these processes would generally act to decrease the dark matter density below what is shown here, particularly in the models with a “spike.”

We will discuss in the next section the prospects of observing DM annihilation radiation from the Galactic center. The dependence of the annihilation signal on

the DM profile is usually contained in the factor J defined as

$$\bar{J}_{\Delta\Omega} = K \Delta\Omega^{-1} \int_{\Delta\Omega} d\psi \int_{\psi} \rho^2 dl \quad (6)$$

with $\Delta\Omega$ the angular acceptance of the detector, dl a distance increment along the line of sight, and ψ the angle between the line of sight and the Galactic center; the normalizing factor K is normally set to $K^{-1} = (8.5\text{kpc})(0.3\text{GeV}/\text{cm}^3)^2$. Henceforth we denote by \bar{J}_3 and \bar{J}_5 the \bar{J} values corresponding to $\Delta\Omega = 10^{-3}$ sr and 10^{-5} sr respectively; the former is the approximate angular acceptance of EGRET⁴⁵ while the latter corresponds approximately to atmospheric Cerenkov telescopes (ACTs) like VERITAS⁴⁶, CANGAROO⁴⁷ and HESS⁴⁸ and to the proposed satellite observatory GLAST.⁴⁹

In dark matter models with an inner spike it is possible to solve analytically the integral of ρ^2 , and the resulting expression for J is

$$\begin{aligned} \bar{J}_{\Delta\Omega} &\approx \frac{4\pi}{3} \frac{J_0}{\Delta\Omega} \frac{\rho_a^2 r_a^3}{R_\odot^2} \left\{ 1 + \frac{3}{2\gamma_{sp} - 3} \left[1 - \left(\frac{r_a}{r_{sp}} \right)^{2\gamma_{sp}-3} \right] \right\} \\ &\approx \frac{4\pi}{3} \frac{J_0}{\Delta\Omega} \frac{\rho_a^2 r_a^3}{R_\odot^2} \frac{1}{1 - 3/(2\gamma_{sp})} \\ &\approx \frac{10}{\Delta\Omega} \left(\frac{\rho_a}{\rho_\odot} \right)^2 \left(\frac{r_a}{R_\odot} \right)^3 \end{aligned} \quad (7)$$

with r_a the outer radius of the region where the density is limited by self annihilations (Fig. 1); these expressions assume that $\Delta\Omega \gg (r_{sp}/R_\odot)^2$ and the latter two expressions assume $r_a \ll r_{sp}$. A feeling for the range of plausible \bar{J} values can be had by computing the ρ_a and r_a values corresponding to a set of ten, minimal supergravity benchmark models.⁵⁰ Setting $\rho_\odot = 0.3 \text{ GeV cm}^{-3}$ and $\gamma_{sp} = 2.4$, and assuming that the dark matter cusp follows $\rho \propto r^{-1.5}$ outside of the spike and inside the Solar circle (the “adiabatically compressed” version of the SHM, one finds $1.2 \times 10^4 \lesssim \Delta\Omega \bar{J} \lesssim 1.5 \times 10^6$. In the absence of the spike, \bar{J} values are many orders of magnitude lower. Such a wide range of \bar{J} values makes it difficult to constrain m or $\langle\sigma v\rangle$ from a measured annihilation flux or even to conclude that a signal would be detectable.

Fortunately, many of the models in Fig. 1 can be ruled out. Once the dark matter distribution has been set up, it will evolve, due to interactions between dark matter particles, stars, and the SBH. In most (though not all) circumstances, this evolution has the effect of decreasing the dark matter density at $r \lesssim r_h$. The most important evolutionary mechanisms are:

- *Scattering of dark matter particles off of stars.* Stars in the Galactic nucleus have much larger kinetic energies than dark matter particles, and gravitational encounters between the two populations tend to drive them toward mutual equipartition, $(1/2)m_* v_*^2 \approx (1/2)mv^2$. Since the stars are the dominant population (at least at the current epoch), the dark matter heats up,

in a time⁵¹

$$T_{\text{heat}} \approx 10^9 \text{ yr} \times \left(\frac{M_{bh}}{3 \times 10^6 M_{\odot}} \right)^{1/2} \left(\frac{r_h}{2 \text{ pc}} \right)^{3/2} \left(\frac{\tilde{m}_{\star}}{M_{\odot}} \right)^{-1} \quad (8)$$

with m_{\star} the mean stellar mass. This heating tends to lower the dark matter density and leads ultimately (in a time of several T_{heat}) to a density profile of the form $\rho \sim r^{-3/2}$, $r_{\text{Sch}} \lesssim r \lesssim r_h$, i.e. it flattens a pre-existing spike.^{51,53,52} T_{heat} is also roughly the time for exchange of kinetic energy *between* stars, as a result of which the *stellar* density profile itself evolves toward a steady-state form, though with a steeper index $\rho_{\star} \sim r^{-7/4}$.^{54,55} This is probably the origin of the power-law stellar density cusp at the Galactic center (eq. 4); the observed index, -1.4 , is not quite as steep as the theoretical value but is probably consistent given the measurement uncertainties and given that the Galactic center contains stars with a range of masses and luminosities.

Interestingly, even if the stellar and dark matter cusps were once destroyed by the scouring effect of a binary SBH,^{56,33,34} both might have been regenerated by this mechanism. In the case of the stars, as long as the density within the SBH's influence radius remains large enough that the star-star relaxation time is shorter than $\sim 10^{10}$ yr, the $r^{-7/4}$ cusp will re-form via the Bahcall-Wolf mechanism⁵⁴. This is likely to be the case if the mass ratio of the pre-existing binary SBH was extreme, e.g. $\sim 10 : 1$. Once the stellar cusp is back in place, heating of dark matter particles by stars will drive the dark matter towards its steady-state distribution, $\rho \sim r^{-3/2}$, although with a lower normalization than before cusp destruction. While many such evolutionary scenarios are possible (and should be worked out in more detail), the existence of a dense, collisional nucleus of stars like that observed in the Galactic center is strong circumstantial evidence of a steeply-rising *dark* matter density near the SBH.

- *Capture of dark matter within the SBH.* Any dark matter particles on orbits that intersect the SBH are lost in a single orbital period. Subsequently, scattering of dark matter particles off stars drives a continuous flux of dark matter into the SBH.⁵⁷ Changes in orbital angular momentum dominate the flux; in a time T_{heat} , most of the dark matter within r_h will have been lost, although the net change in the dark matter density profile will be more modest than this suggests since more particles are continuously being scattered in.⁵¹
- *Capture of dark matter within stars.* Another potential loss term for the dark matter is capture *within* stars, due to scattering off nuclei followed by annihilation in stellar cores.^{58,59,60} However this process is not likely to be important unless the cross section for WIMP-on-proton scattering is very large.

These effects, as well as dark matter self-annihilations, can be modelled in a time-dependent way via the orbit-averaged Fokker-Planck equation:⁵¹

$$\frac{\partial f}{\partial t} = -\frac{1}{4\pi^2 p} \frac{\partial F_E}{\partial E} - f(E)\nu_{\text{coll}}(E) - f(E)\nu_{\text{lc}}(E) \quad (9)$$

with $f(E)$ the phase-space mass density of dark matter, $E \equiv -v^2/2 + \phi(r)$ the energy per unit mass of a dark-matter particle, and $\phi(r)$ the gravitational potential generated by the stars and SBH. The terms on the right-hand side of Eq. (9) describe the diffusion of dark matter particles in phase space due to scattering off stars (F_E); loss of dark matter due to self-annihilations and/or capture within stars (ν_{coll}); and the loss-cone flux into the SBH (ν_{lc}). Eq. (9) assumes an isotropic distribution of dark-matter velocities; this assumption is likely to break down very near the SBH, but the angular-momentum dependence of the loss cone flux is well understood and can be approximated via an energy-dependent loss term $\nu_{\text{lc}}(E)$.⁵¹

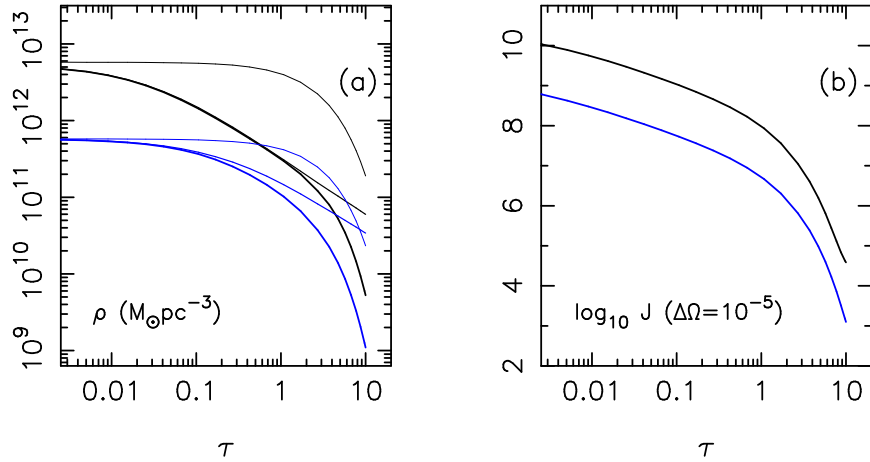


Fig. 2. (a) Evolution of the dark matter density at a radius of $10^{-5}r_h \approx 2 \times 10^{-5} \text{pc}$ from the center of the Milky Way due to the physical processes discussed in the text (Eq. 9). Initial conditions were the standard halo model discussed in the text plus spike; the upper(lower) set of curves correspond to an initial density normalization at r_h of $10(100)M_\odot \text{pc}^{-3}$. Mass and annihilation cross section of the dark matter particles were set to $m = 200 \text{ GeV}$, $\langle\sigma v\rangle = 10^{-27} \text{cm}^3 \text{s}^{-1}$. In order of increasing thickness, the curves show the evolution of ρ in response to heating by stars; to self-annihilations; and to both processes acting together. Time is in units of T_{heat} defined in the text; $\tau = 10$ corresponds roughly to 10^{10} yr . (b) Evolution of \bar{J} averaged over an angular window of 10^{-5} sr .

Fig. 2a shows the evolution of the dark matter density computed in this way, starting from a $\rho \sim r^{-2.33}$ spike ($\rho \sim r^{-1}$ cusp). Two values were taken for the initial density normalization at $r = r_h$, $\rho(r_h) = (10, 100)M_\odot \text{pc}^{-3}$; these values bracket the value $\rho(r_h) \approx 30M_\odot \text{pc}^{-3}$ obtained by extrapolating the SHM inwards from the Solar circle with $\rho(R_\odot) = 0.3 \text{ GeVcm}^{-3}$ (Fig. 1). The self-annihilation

term in Eq. (9) was computed assuming $m = 200$ GeV, $\langle\sigma v\rangle = 10^{-27}\text{cm}^3\text{s}^{-1}$. The early evolution is dominated by self-annihilations but for $t \gtrsim 10^9\text{yr} \approx T_{\text{heat}}$, heating of dark matter by stars dominates. The change in $\bar{J}(\Delta\Omega = 10^{-5})$ (Fig. 2b.) is dramatic, with final values in the range $10^4 \lesssim \bar{J} \lesssim 10^5$.

4. Direct and Indirect Detection

In order to understand the nature of the dark matter, it is crucial to search for non-gravitational signatures. Physics beyond the standard model is actively being investigated using accelerators, and this is one of the main goals of the upcoming Large Hadron Collider (LHC), expected to begin operation around 2007 with proton-proton collisions at center-of-mass energies of 14 TeV. Numerous classes of models which provide interesting dark matter candidates will be tested at the LHC (Refs. 61 – 69).

An alternative approach is provided by so-called *direct detection* experiments. If the Galaxy is filled with WIMPs, then many of them should pass through the Earth, making it possible to look for the interaction of such particles with baryonic matter, e.g. by recording the recoil energy of nuclei as WIMPs scatter off them.^{70,71} The signal in this case depends on the density and velocity distribution of WIMPs in the solar neighborhood and on the WIMP-nucleon scattering cross section. WIMPs can couple either with the spin content of a nucleus, through axial-vector (spin dependent) interactions, or with the nuclear mass, through scalar (spin-independent) scattering. The second interaction typically dominates over spin-dependent scattering in current experiments, which use heavy atoms as targets. More than 20 direct dark matter detection experiments are either now operating or are currently in development. Presently, the best direct detection limits come from the CDMS⁷² and Edelweiss⁷³ experiments, which probe nucleon-WIMP scattering cross sections of order 10^{-7}pb , for a WIMP mass of order 100 GeV. These experiments have ruled out the WIMP discovery claimed by the DAMA collaboration,⁷⁴ although it may still be possible to find exotic particle candidates and Galaxy halo models which are able to accommodate the data from all current experiments.^{75,76,77}

Alternatively, dark matter can be searched for *indirectly*, via the study of the local flux of positrons and antiprotons. In fact, if the paradigm of WIMPs as massive particles in thermal equilibrium in the early universe is correct, dark matter particles are expected to annihilate in the Galactic halo producing possibly large fluxes of secondary particles. The High Energy Antimatter Telescope (HEAT) observed a flux of cosmic positrons well in excess of the predicted rate, peaking around $\sim 10\text{GeV}$ and extending to higher energies,⁷⁸ which could be the product of dark matter annihilations if sufficient clumping were present in the halo (Refs. 79 – 86). Upcoming experiments, such as AMS-02,⁸⁷ PAMELA,⁸⁸ and Bess Polar,⁸⁹ will refine the positron spectrum considerably. An antiproton signal could also provide a signature of dark matter.^{90,91,92}

Unlike other secondary particles, neutrinos produced by dark matter annihila-

tions can escape from dense media in which such annihilations may take place. For example, WIMPs that are captured in the Sun or Earth can annihilate at great rates. Although gamma rays cannot escape these objects, neutrinos often can, providing an interesting signature to search for with high-energy neutrino telescopes (Refs. 93 – 101). Although strongly model-dependent, the limits on the neutrino flux can be used to set constraints on dark matter particles.

Dark matter could also be indirectly detected through its annihilation radiation in the Galactic halo or in extra-galactic sources. The prospects of detecting synchrotron radiation due to dark matter annihilations in the Galactic center have been studied in Refs. 102 – 104, while Ref. 105 contains a discussion of the prospects for detecting the neutrino flux. Annihilation radiation could be enhanced by the presence of substructures in the Galactic halo, either “clumps” (Refs. 106 – 112) or “caustics” (Refs. 113 – 115). Recently, high-resolution numerical simulations have pointed to the existence of mini-halos with masses as small as 10^{-6} solar masses and sizes as small as the solar system¹¹⁶ (see also Refs. 117, 118). If confirmed, this could have important consequences for indirect DM searches, and certainly deserves further investigation.

The gamma-ray extra-galactic background produced by dark matter annihilations taking place in all structures and substructures in the Universe has been investigated in Refs. 119 – 121. One usually finds that the prospects to observe this signal are less promising than in the case of the gamma-rays from the Galactic center however (see e.g. Ref. 124).

Much attention has been devoted to the study of gamma-rays from dark matter annihilations in the Galactic center (Refs. 122 – 127). Given a detector with angular acceptance $\Delta\Omega$ sr, the observed flux of photons produced by annihilations of dark matter particles of mass m and density ρ is¹²³

$$\Phi(\Delta\Omega, E) = \Delta\Omega \frac{dN}{dE} \frac{\langle\sigma v\rangle}{4\pi m^2} \bar{J}_{\Delta\Omega} \quad (10)$$

where dN/dE is the spectrum of secondary photons per annihilation, $\langle\sigma v\rangle$ is the velocity-averaged self-annihilation cross section, dl is an element of length along the line of sight and $\bar{J}_{\Delta\Omega}$ was defined in Eq. (6). The flux from solid angle $\Delta\Omega$ is then

$$\Phi(\Delta\Omega, E) \approx 1.9 \times 10^{-12} \frac{dN}{dE} \frac{\langle\sigma v\rangle}{10^{-26} \text{cm}^3 \text{s}^{-1}} \left(\frac{1 \text{TeV}}{m} \right)^2 \bar{J}_{\Delta\Omega} \Delta\Omega \text{cm}^{-2} \text{s}^{-1}. \quad (11)$$

Inward extrapolation of the density of the standard halo model (SHM) from the Solar circle into the Galactic center gives $\bar{J}_3 \approx 10^2$ and $\bar{J}_5 \approx 10^3$. These \bar{J} -values are large enough to produce observable signals for many interesting choices of $\langle\sigma v\rangle$ and m . On the other hand, a recent detection¹³² by ACTs of a Galactic center gamma-ray source with energies up to 10 TeV requires \bar{J} values that are 10^2 to 10^4 times bigger than in the SHM,^{128,129} assuming that the signal comes from dark matter annihilations. Achieving such large \bar{J} values without abandoning the Λ CDM paradigm would require a significant enhancement in the dark matter density very

near the Galactic center, for instance, in the form of a density “spike” near the SBH.

As discussed in §3, a steeply-rising dark matter density will due to self-annihilations and to dynamical interactions with the baryons. The results from a large set of time integrations of Eq. (9) are summarized in Table 1. Two extreme particle physics models were considered. In the first case, in order to maximize the ratio $\langle\sigma v\rangle/m$, a cross section $\langle\sigma v\rangle_{\text{th}} = 3 \times 10^{-26} \text{ cm}^3 \text{ s}^{-1}$ was assumed and m was set to 50 GeV. Higher values of $\langle\sigma v\rangle$, though possible, would imply a low relic density, making the candidate a subdominant component of the dark matter in the universe. The lower limit on the mass strictly applies only to neutralinos in theories with gaugino and sfermion mass unification at the GUT scale,¹³⁰ while the limit on the mass of KK particles is higher. The second extreme case assumed $\langle\sigma v\rangle = 0$. Table 1 gives values of $\bar{J}(\Delta\Omega = 10^{-3})$ and $\bar{J}(\Delta\Omega = 10^{-5})$ at $\tau = 10$ for each of these extreme particle physics models and for a variety of initial conditions. The final \bar{J} -values depend appreciably on the particle physics model only when the initial dark matter density has a spike around the SBH; in other cases the central density is too low for annihilations to affect \bar{J} . Particularly in the case of maximal $\langle\sigma v\rangle$, the final \bar{J} values are modest, $\log_{10} \bar{J}_3 \lesssim 5.3$ and $\log_{10} \bar{J}_5 \lesssim 7.0$, compared with the much larger values at $\tau = 0$ in the presence of spikes.

Table 1. Results of time-integrations of Eq. (9) from a variety of initial dark matter models. γ_c and γ_{sp} are the power-law indices of the initial cusp and spike respectively. r_c is the dark matter core radius in units of $r_h \approx 2 \text{ pc}$; $\rho \propto r^{-1/2}$ for $r_{sp} < r < r_c$. Density at R_\odot is in units of GeV cm^{-3} . \bar{J}_3 and \bar{J}_5 are values of \bar{J} averaged over windows of solid angle 10^{-3} sr and 10^{-5} sr respectively and normalized as described in the text. The final two columns give \bar{J} in evolved models for $\langle\sigma v\rangle = 0$ (no annihilations) and for $(\langle\sigma v\rangle, M) = (3 \times 10^{-26} \text{ cm}^3 \text{ s}^{-1}, 50 \text{ GeV})$ (maximal annihilation rate), respectively.

Model	γ_c	γ_{sp}	r_c	$\rho(R_\odot)$	$\log_{10} \bar{J}_3 (\bar{J}_5)$		
					$\tau = 0$	$\tau = 10$	$\tau = 10$
1	1.0	—	—	0.3	2.56(3.51)	2.56(3.50)	2.56(3.50)
2	1.0	—	—	0.5	3.00(3.96)	3.00(3.94)	3.00(3.94)
3	1.0	—	10	0.3	2.54(3.33)	2.54(3.33)	2.54(3.33)
4	1.0	—	100	0.3	2.38(2.65)	2.38(2.65)	2.38(2.65)
5	1.0	2.33	—	0.3	9.21(11.2)	3.86(5.84)	2.56(3.52)
6	1.0	2.33	—	0.5	9.65(11.7)	4.31(6.29)	3.00(3.96)
7	1.0	2.29	10	0.3	6.98(8.98)	2.61(3.88)	2.54(3.33)
8	1.0	2.29	100	0.3	5.98(7.98)	2.39(2.99)	2.38(2.65)
9	1.5	—	—	0.3	5.36(7.30)	4.81(6.58)	4.78(6.53)
10	1.5	—	—	0.5	5.80(7.75)	5.26(7.03)	5.23(6.98)
11	1.5	—	10	0.3	4.51(5.82)	4.51(5.82)	4.51(5.82)
12	1.5	—	100	0.3	3.85(4.23)	3.85(4.23)	3.85(4.23)
13	1.5	2.40	—	0.3	14.3(16.3)	8.81(10.8)	4.81(6.58)
14	1.5	2.40	—	0.5	14.8(16.8)	9.25(11.3)	5.25(7.02)
15	1.5	2.29	10	0.3	9.67(11.7)	4.77(6.51)	4.51(5.82)
16	1.5	2.29	100	0.3	7.67(9.67)	3.87(4.64)	3.86(4.23)

Table 2. Parameters in the fitting function for the boost.

Model	$\Delta\Omega = 10^{-3}$				$\Delta\Omega = 10^{-5}$			
	B_{min}	B_{max}	a	b	B_{min}	B_{max}	a	b
5	-0.02	1.31	0.66	0.73	-0.05	2.35	0.55	1.50
6	-0.01	1.31	0.66	0.51	-0.06	2.34	0.56	1.28
7	-0.02	0.05	0.75	0.92	-0.18	0.38	0.72	1.31
8	-0.18	-0.17	0.76	1.37	-0.86	-0.51	0.73	1.64
13	2.14	6.28	0.42	-0.05	2.95	7.35	0.40	0.10
14	2.16	6.29	0.43	-0.28	2.97	7.36	0.41	0.13
15	1.96	2.21	0.74	-0.27	2.32	3.02	0.71	0.07
16	1.30	1.31	0.75	0.53	0.73	1.14	0.73	0.84

In these evolutionary models, the value of \bar{J} at a fixed time $t = \tau T_{\text{heat}}$ is determined completely by the initial conditions and by the quantity $\langle\sigma v\rangle/m$ that specifies the annihilation rate. This outcome can be expressed in terms of the *boost factor* b defined as \bar{J}/\bar{J}_N , with \bar{J}_N the value in the SHM having the same density normalization at $r = R_\odot$ as in the evolving model. One finds¹³¹ that the boost factors at $\tau = 10$ (roughly 10^{10} yr) can be well approximated by the function

$$B(X) = B_{max} - (1/2)(B_{max} - B_{min})\{1 + \tanh[a(X - b)]\} \quad (12)$$

with $X \equiv \log_{10}(\langle\sigma v\rangle/10^{-30}\text{cm}^3\text{s}^{-1})/(m/100\text{GeV})$ and $B \equiv \log_{10} b$. Values of the fitting parameters are given in Table 2 for the “spike” models of Table 1; as noted above, in the absence of a spike, the final \bar{J} values are essentially unaffected by annihilations hence independent of $\langle\sigma v\rangle/m$. Recent analyses^{128,129} of the HESS Galactic center data¹³² suggest that the observed gamma-ray spectrum is consistent with particle masses of order 10 TeV and cross sections of order $3 \times 10^{-26}\text{cm}^3\text{s}^{-1}$, if boost factors are as high as $10^3 \lesssim b \lesssim 10^4$. Table 2 shows that such boost factors are indeed achievable at $X = \log_{10}(3 \times 10^{-26}/10^{-30})/(10^4/100) \approx 2.5$ if the initial dark matter distribution is similar to that of Models 13 or 14, i.e. a “spike” inside of a $\rho \sim r^{-1.5}$ cusp.

Annihilation radiation might also be detected from the centers of galaxies other than the Milky Way (Refs. 133 – 143). Even globular clusters¹⁴⁴ have been suggested as possible targets. As in the case of the Milky Way, the major uncertainty in predictions of the annihilation flux from external galaxies is the unknown distribution of dark matter on small scales; absent power-law cusps or spikes, indirect detection of dark matter from external galaxies is probably impossible with the current generation of detectors.¹⁴³ As argued above, a plausible guide to the dark matter distribution on small scales is the *stellar* density profile. The Local Group galaxies M31 and M32 both exhibit steep stellar cusps, $\rho_\star \sim r^{-\gamma_\star}$, $1.5 \lesssim \gamma_\star \lesssim 2.0$, inward of ~ 1 pc, similar to what is observed in the Milky Way;¹⁴⁵ these galaxies also show clear kinematical evidence for SBHs. By contrast, the Local Group galaxies M33 and NGC205 exhibit cores in the stellar density and any SBHs in these galaxies are too small to be detected.^{146,147} Stellar cusps like the one in the Milky Way would be unresolved at the distance of the Virgo cluster, but it is a reasonable

guess that all comparably-luminous galaxies contain similar distributions of luminous and dark matter on sub-parsec scales. The situation is likely to be different for giant galaxies like M87 in Virgo, which are known to have much shallower stellar density profiles within their SBH's sphere of influence, probably a consequence of an earlier epoch of scouring by binary SBHs.¹⁴⁸ The matter distribution near the centers of giant galaxies is probably essentially unchanged since the last round of galaxy mergers, making them unfelicitous sites for indirect detection of dark matter.

Acknowledgments

GB is supported by the DOE and the NASA grant NAG 5-10842 at Fermilab. DM acknowledges support from the NSF (AST-0206031, AST-0420920 and AST-0437519), NASA (NNG04GJ48G) and the Space Telescope Science Institute (HST-AR-09519.01-A and HST-GO-09401.10A).

References

1. D. N. Spergel *et al.*, *Astrophys. J. Suppl.* **148**, 175 (2003) [arXiv:astro-ph/0302209].
2. K. A. Olive, TASI lectures on dark matter, arXiv:astro-ph/0301505.
3. G. Bertone, D. Hooper and J. Silk, *Phys. Rept.* **405** (2005) 279 [arXiv:hep-ph/0404175].
4. L. Bergstrom, *Rept. Prog. Phys.* **63** (2000) 793 [arXiv:hep-ph/0002126].
5. T. Appelquist, H. C. Cheng and B. A. Dobrescu, *Phys. Rev. D* **64**, 035002 (2001) [arXiv:hep-ph/0012100].
6. H. C. Cheng, K. T. Matchev and M. Schmaltz, *Phys. Rev. D* **66**, 036005 (2002) [arXiv:hep-ph/0204342].
7. G. Servant and T. M. Tait, *Nucl. Phys. B* **650** (2003) 391 [arXiv:hep-ph/0206071].
8. B. W. Lee and S. Weinberg, *Phys. Rev. Lett.* **39**, 165 (1977).
9. P. Hut, *Phys. Lett. B* **69** (1977) 85.
10. S. Weinberg, 1995, *The Quantum Theory of Fields Vol 1: Foundations*, Cambridge University Press.
11. K. Griest and M. Kamionkowski, *Phys. Rev. Lett.* **64** (1990) 615.
12. C. Boehm, T. A. Ensslin and J. Silk, arXiv:astro-ph/0208458.
13. C. Boehm and P. Fayet, arXiv:hep-ph/0305261.
14. P. Jean *et al.*, "Early SPI/INTEGRAL measurements of galactic 511 keV line emission from positron annihilation," *Astron. Astrophys.* **407**, L55 (2003) [arXiv:astro-ph/0309484].
15. J. Knodlseder *et al.*, "Early SPI/INTEGRAL constraints on the morphology of the 511 keV line emission in the 4th galactic quadrant," arXiv:astro-ph/0309442.
16. G. Weidenspointner *et al.*, "SPI observations of positron annihilation radiation from the 4th galactic quadrant: sky distribution," arXiv:astro-ph/0406178.
17. J. F. Beacom, N. F. Bell and G. Bertone, arXiv:astro-ph/0409403.
18. C. Boehm and Y. Ascasibar, *Phys. Rev. D* **70** (2004) 115013 [arXiv:hep-ph/0408213].
19. C. Boehm, *Phys. Rev. D* **70** (2004) 055007 [arXiv:hep-ph/0405240].
20. D. J. H. Chung, P. Crotty, E. W. Kolb and A. Riotto, *Phys. Rev. D* **64** (2001) 043503 [arXiv:hep-ph/0104100].
21. S. Chang, C. Coriano and A. E. Faraggi, *Nucl. Phys. B* **477**, 65 (1996) [arXiv:hep-ph/9605325].
22. J. R. Primack, in *Proceedings of the Fifth International UCLA Symposium on Sources and Detection of Dark Matter*, *Nucl. Phys. B. Proc. Suppl.* **124**, 3 (astro-ph/0205391)

23. M. Merrifield, in *International Astronomical Union Symposium no. 220*, eds. S. D. Ryder *et al.* (Astronomical Society of the Pacific, 2004), p. 431
24. J. N. Navarro, in *International Astronomical Union Symposium no. 220*, eds. S. D. Ryder *et al.* (Astronomical Society of the Pacific, 2004), p. 61
25. J. F. Navarro *et al.*, *Mon. Not. R. Astron. Soc.* **349**, 1039 (2004).
26. D. Reed, F. Governato, L. Verde, J. Gardner, T. Quinn, J. Stadel, J., D. Merritt, G. Lake, *Mon. Not. R. Astron. Soc.* **357**, 82 (2005)
27. D. Merritt, J. Navarro, A. Ludlow, and A. Jenkins, astro-ph/0502515 (2005)
28. J. F. Navarro, C. S. Frenk, and S. D. M. White, *Astrophys. J.* **462**, 563 (1996).
29. G. R. Blumenthal, S. M. Faber, R. Flores, and J. R. Primack, *Astrophys. J.* **301**, 27 (1986).
30. J. Edsjo, M. Schelke, and P. Ullio, astro-ph/0405414.
31. F. Prada, A. Klypin, J. Flix, M. Martinez, and E. Simonneau, *Phys. Rev. Lett.* **93**, 241301 (2004).
32. O. Y. Gnedin, A. V. Kravtsov, A. A. Klypin, and D. Nagai, *Astrophys. J.* **616**, 16 (2004).
33. P. Ullio, H.-Z. Zhao, and M. Kamionkowski, *Phys. Rev. D.*, **64**, 043504 (2001).
34. D. Merritt, M. Milosavljevic, L. Verde, and R. Jimenez, *Phys. Rev. Lett.* **88**, 191301 (2002).
35. D. Merritt and M. Milosavljevic, in *Dark Matter in Astro- and Particle Physics*, eds. H. V. Klapdor-Kleingrothaus and R. D. Viollier (Springer, 2002), p. 79.
36. R. Genzel *et al.*, *Astrophys. J.* **594**, 812 (2003).
37. D. Chakrabarty and P. Saha, *Astronom. J.* **122**, 232 (2001).
38. A. M. Ghez *et al.* *Astrophys. J.* **586**, L127 (2003).
39. R. Schoedel, R. Genzel, T. Ott, A. Eckart, N. Mouawad and T. Alexander, *Astrophys. J.* **596**, 1015 (2003).
40. P. J. E. Peebles, *Gen. Rel. Grav.* **3**, 61 (1972).
41. P. J. Young, *Astrophys. J.* **242**, 1232 (1980)
42. P. Gondolo and J. Silk, *Phys. Rev. Lett.* **83**, 1719 (1999).
43. D. Merritt, in *Carnegie Observatories Astrophysics Series, Vol. 1: Coevolution of Black Holes and Galaxies*, ed. L. C. Ho (Cambridge: Cambridge Univ. Press), in press (2004).
44. V. Berezinsky, A. Bottino, and G. Mignola, *Phys. Lett. B* **325**, 136 (1994).
45. <http://coss.gsfc.nasa.gov/egret/>
46. <http://veritas.sao.arizona.edu/>
47. <http://icrhp9.icrr.u-tokyo.ac.jp/>
48. <http://www.mpi-hd.mpg.de/hfm/HESS/HESS.html/>
49. <http://www-glast.stanford.edu/>
50. M. Battaglia, A. De Roeck, J. R. Ellis, F. Gianotti, K. A. Olive, and L. Pape, *Eur. Phys. J. C* **33**, 273 (2004).
51. D. Merritt, *Phys. Rev. Lett.* **92**, 201304 (2004).
52. A. S. Ilyin, K. P. Zybin, and A. V. Gurevich, *Zh. Eksp. Teor. Fiz.* **98**, 5 (2004).
53. O. Y. Gnedin and J. R. Primack, *Phys. Rev. Lett.* **93**, 061302 (2004).
54. J. N. Bahcall and S. Wolf, *Astrophys. J.* **209**, 214 (1976).
55. M. Preto, D. Merritt, and R. Spurzem, *Astrophys. J.* **613**, L109 (2004).
56. M. Milosavljevic and D. Merritt, *Astrophys. J.*, **563**, 34 (2001).
57. V. S. Berezinsky, A. V. Gurevich, and K. P. Zybin, *Phys. Lett. B* **294**, 221 (1994).
58. W. H. Press and D. N. Spergel, *Astrophys. J.* **296**, 679 (1985).
59. P. Salati and J. Silk, *Astrophys. J.* **338**, 24 (1989).
60. A. Bouquet, P. Salati, and J. Silk, *Phys. Rev. D* **40**, 3168 (1989).
61. ATLAS TDR, report CERN/LHCC/99-15 (1999).

62. CMS TP, report CERN/LHCC/94-38 (1994).
63. S. Dawson, E. Eichten and C. Quigg, Phys. Rev. D **31**, 1581 (1985).
64. B. C. Allanach *et al.* [Beyond the Standard Model Working Group Collaboration], “Les Houches ‘Physics at TeV Colliders 2003’ Beyond the Standard Model Working Group: Summary report”, arXiv:hep-ph/0402295.
65. B. C. Allanach, C. G. Lester, M. A. Parker and B. R. Webber, JHEP **0009**, 004 (2000) [arXiv:hep-ph/0007009].
66. H. Baer, C. Balazs, A. Belyaev, T. Krupovnickas and X. Tata, JHEP **0306**, 054 (2003) [arXiv:hep-ph/0304303].
67. I. Hinchliffe, F. E. Paige, M. D. Shapiro, J. Soderqvist and W. Yao, Phys. Rev. D **55**, 5520 (1997) [arXiv:hep-ph/9610544].
68. G. Polesello and D. R. Tovey, arXiv:hep-ph/0403047.
69. A. Birkedal, K. Matchev and M. Perelstein, arXiv:hep-ph/0403004.
70. A. Drukier and L. Stodolsky, Phys. Rev. D **30**, 2295 (1984).
71. M. W. Goodman and E. Witten, Phys. Rev. D **31**, 3059 (1985).
72. D. S. Akerib *et al.* [CDMS Collaboration], Phys. Rev. D **68** (2003) 082002 [arXiv:hep-ex/0306001].
73. A. Benoit *et al.*, Phys. Lett. B **545** (2002) 43 [arXiv:astro-ph/0206271].
74. R. Bernabei *et al.*, *Talk at the 10th International Workshop on Neutrino Telescopes, Venice, Italy*, (2003), [arXiv:astro-ph/0305542].
75. G. Prezeau, A. Kurylov, M. Kamionkowski and P. Vogel, Phys. Rev. Lett. **91**, 231301 (2003) [arXiv:astro-ph/0309115].
76. G. Gelmini and P. Gondolo, arXiv:hep-ph/0405278.
77. D. Tucker-Smith and N. Weiner, arXiv:hep-ph/0402065.
78. S. W. Barwick *et al.* [HEAT Collaboration], Astrophys. J. **482**, L191 (1997) [arXiv:astro-ph/9703192].
79. G. L. Kane, L. T. Wang and J. D. Wells, Phys. Rev. D **65**, 057701 (2002).
80. M. Kamionkowski and M. S. Turner, Phys. Rev. D **43**, 1774 (1991).
81. E. A. Baltz, J. Edsjo, K. Freese and P. Gondolo, Phys. Rev. D **65** (2002) 063511 [arXiv:astro-ph/0109318].
82. M. S. Turner and F. Wilczek, Phys. Rev. D, **42**, 1001 (1990).
83. A. J. Tylka, Phys. Rev. Lett., **63**, 840 (1989).
84. G. L. Kane, L. T. Wang and T. T. Wang, Phys. Lett. B **536**, 263 (2002).
85. E. A. Baltz and J. Edsjo, Phys. Rev. D **59** (1999) 023511 [arXiv:astro-ph/9808243].
86. H. C. Cheng, J. L. Feng and K. T. Matchev, Phys. Rev. Lett. **89**, 211301 (2002) [arXiv:hep-ph/0207125].
87. R. Battiston, *Frascati Physics Series* **24**, 261.
88. <http://www.cerncourier.com/main/article/42/8/17>
89. T. Sanuki, Int. J. Mod. Phys. A **17**, 1635 (2002).
90. A. Bottino, F. Donato, N. Fornengo and P. Salati, Phys. Rev. D **58**, 123503 (1998).
91. F. Donato, N. Fornengo, D. Maurin, P. Salati and R. Taillet, arXiv:astro-ph/0306207.
92. L. Bergstrom, J. Edsjo and P. Ullio, arXiv:astro-ph/9902012.
93. J. Silk, K. Olive and M. Srednicki, Phys. Rev. Lett. **55**, 257 (1985).
94. F. Halzen, T. Stelzer and M. Kamionkowski, Phys. Rev. D **45**, 4439 (1992).
95. J. L. Feng, K. T. Matchev and F. Wilczek, Phys. Rev. D **63**, 045024 (2001).
96. V. D. Barger, F. Halzen, D. Hooper and C. Kao, Phys. Rev. D **65**, 075022 (2002).
97. V. Berezhinsky, A. Bottino, J. Ellis, N. Fornengo, G. Mignola and S. Scopel, *Astropart. Phys.* **5**, 333 (1996) [hep-ph/9603342].
98. L. Bergstrom, J. Edsjo and P. Gondolo, Phys. Rev. D **58** (1998) 103519 [arXiv:hep-ph/9806293].

99. K. Freese, *Phys. Lett. B* **167**, 295 (1986).
100. L. M. Krauss, M. Srednicki and F. Wilczek, *Phys. Rev. D* **33**, 2079 (1986).
101. T. K. Gaisser, G. Steigman and S. Tilav, *Phys. Rev. D* **34**, 2206 (1986).
102. P. Gondolo, *Phys. Lett. B* **494**, 181 (2000).
103. G. Bertone, G. Servant and G. Sigl, *Phys. Rev. D* **68** (2003) 044008 [arXiv:hep-ph/0211342].
104. R. Aloisio, P. Blasi and A. V. Olinto, *JCAP* **0405**, 007 (2004) [arXiv:astro-ph/0402588].
105. G. Bertone, E. Nezri, J. Orloff and J. Silk, *Phys. Rev. D* **70**, 063503 (2004) [arXiv:astro-ph/0403322].
106. L. Bergstrom, J. Edsjo and P. Ullio, *Phys. Rev. D* **58** (1998) 083507 [arXiv:astro-ph/9804050].
107. C. Calcaneo-Roldan and B. Moore, *Phys. Rev. D* **62** (2000) 123005 [arXiv:astro-ph/0010056].
108. A. Tasitsiomi and A. V. Olinto, *Phys. Rev. D* **66** (2002) 083006 [arXiv:astro-ph/0206040].
109. V. Berezhinsky, V. Dokuchaev and Y. Eroshenko, *Phys. Rev. D* **68** (2003) 103003 [arXiv:astro-ph/0301551].
110. F. Stoehr, S. D. White, V. Springel, G. Tormen and N. Yoshida, *Mon. Not. Roy. Astron. Soc.* **345**, 1313 (2003) [arXiv:astro-ph/0307026].
111. P. Blasi, A. V. Olinto and C. Tyler, *Astropart. Phys.* **18**, 649 (2003) [arXiv:astro-ph/0202049].
112. S. M. Koushiappas, A. R. Zentner and T. P. Walker, *Phys. Rev. D* **69**, 043501 (2004) [arXiv:astro-ph/0309464].
113. P. Sikivie, *Phys. Rev. D* **60** (1999) 063501 [arXiv:astro-ph/9902210].
114. L. Bergstrom, J. Edsjo and C. Gunnarsson, *Phys. Rev. D* **63** (2001) 083515 [arXiv:astro-ph/0012346].
115. R. Mohayaee and S. Shandarin, arXiv:astro-ph/0503163.
116. J. Diemand, B. Moore and J. Stadel, *Nature* **433** (2005) 389.
117. A. M. Green, S. Hofmann and D. J. Schwarz, arXiv:astro-ph/0503387.
118. A. Loeb and M. Zaldarriaga, arXiv:astro-ph/0504112.
119. L. Bergstrom, J. Edsjo and P. Ullio, *Phys. Rev. Lett.* **87** (2001) 251301 [arXiv:astro-ph/0105048].
120. J. E. Taylor and J. Silk, *Mon. Not. Roy. Astron. Soc.* **339** (2003) 505 [arXiv:astro-ph/0207299].
121. P. Ullio, L. Bergstrom, J. Edsjo and C. Lacey, *Phys. Rev. D* **66** (2002) 123502 [arXiv:astro-ph/0207125].
122. F. W. Stecker, *Phys. Lett. B* **201**, 529 (1988).
123. L. Bergstrom, P. Ullio and J. H. Buckley, *Astropart. Phys.* **9**, 137 (1998).
124. S. Ando, arXiv:astro-ph/0503006.
125. G. Bertone, G. Sigl and J. Silk, *Mon. Not. Roy. Astron. Soc.* **326** (2001) 799 [arXiv:astro-ph/0101134].
126. A. Cesarini, F. Fucito, A. Lionetto, A. Morselli and P. Ullio, *Astropart. Phys.* **21**, 267 (2004) [arXiv:astro-ph/0305075].
127. N. Fornengo, L. Pieri and S. Scopel, *Phys. Rev. D* **70** (2004) 103529 [arXiv:hep-ph/0407342].
128. L. Bergstrom, T. Bringmann, M. Eriksson, and M. Gustafsson, astro-ph/0410359.
129. D. Hooper and J. March-Russell, hep-ph/0412048.
130. S. Eidelman *et al.*, *Phys. Lett. B* **592**, 1 (2004).
131. G. Bertone and D. Merritt, astro-ph/0501000

- 132. F. A. Aharonian *et al.*, *Astron. Astrophys.* **425**, L13 (2004).
- 133. P. Gondolo, *Nucl. Phys. B (Proc. Suppl)* **35**, 148 (1994).
- 134. E. A. Baltz, C. Briot, P. Salati, R. Taillet, and J. Silk, *Phys. Rev. D.* **61**, 023514 (1999).
- 135. C. Tyler, *Phys. Rev. D* **66**, 023509 (2002).
- 136. F. A. Aharonian *et al.*, *Astron. Astrophys.* **400**, 153 (2003).
- 137. A. Falvard *et al.*, *Astropart. Phys.* **20**, 467 (2003).
- 138. V. V. Vassiliev *et al.*, in *Proceedings of the 28th International Cosmic Ray Conference* eds. (Universal Academy Press, 2003).
- 139. L. Pieri and E. Branchini, *Phys. Rev. D* **69**, 043512 (2004).
- 140. N. Fornengo, L. Pieri, and S. Scopel, *Phys. Rev. D.* **70**, 103529 (2004).
- 141. A. Tasitsiomi, J. Gaskins, and A. V. Olinto, *Astropart. Phys.* **21**, 637
- 142. D. Hooper *et al.*, *Phys. Rev. Lett.* **93**, 161302 (2004).
- 143. N. W. Evans, F. Ferrer, and S. Sarker, *Phys. Rev. D* **69**, 123501 (2004).
- 144. E. Giraud *et al.*, in *Astronomy, Cosmology and Fundamental Physics, Proceedings of the ESO-CERN-ESA Symposium*, eds. P. A. Shaver, L. Di Lella, and A. Gimenez (Springer, 2003).
- 145. T. R. Lauer, S. M. Faber, E. A. Ajhar, C. J. Grillmair, and P. A. Scowen, *Astron. J.* **116**, 2263 (1998).
- 146. D. Merritt, L. Ferrarese, and C. L. Joseph, *Science*, **293**, 1116 (2001).
- 147. M. Valluri, L. Ferrarese, D. Merritt, and C. L. Joseph, astro-ph/0502493 (2005).
- 148. M. Milosavljević, D. Merritt, A. Rest, and F. van den Bosch, *Mon. Not. R. Astron. Soc.* **331**, L51 (2002).